

Methods for quantification of cerebral glycolytic metabolism using 2-deoxy-2-[¹⁸F]fluoroglucose in small animals

Silvana Prando^{1*}, Carla Rachel Ono¹, Cecil Chow Robilotta², Marcelo Tatit Sapienza¹

¹ Nuclear Medicine Center, School of Medicine, University of São Paulo, São Paulo, SP, Brazil.

² Institute of Physics, University of São Paulo, São Paulo, SP, Brazil.

Abstract Introduction: The use of the same imaging and quantification techniques in small animals and clinical studies presents the opportunity for direct translational research in drug discovery and development, in neuropharmacological basis of neurological and psychiatric diseases, and in optimization of drug therapy. Thus, positron emission tomography (PET) studies in rodents can bridge the gap between pre-clinical and clinical research. The aim should be to find a method with capability to measure, without compromising accuracy, glucose distribution in the structures of the brain, which can also be used in pathological situations and with applicability for other substances than glucose analogue. **Methods:** This is a systematic review of several assessment techniques available, including visual and quantitative methods that enable the investigation of the transport mechanisms and enzymes involved in glucose metabolism in the brain. In addition to the ex vivo methods, PET with glucose analogues allows in vivo analyses using qualitative, semiquantitative and quantitative methods. **Results:** These techniques provide different results, and the applicability of a specific method is related to the purpose of the study and the multiple factors that may interfere in the process. **Conclusion:** This review provides a solid background of tools and quantification methods for medical physicists and other professionals interested in cerebral glycolytic metabolism quantification in experimental animals. It also addresses the main factors related to animals, equipment and techniques that are used, as well as how these factors should be understood to better interpret the results obtained from experiments.

Keywords Nuclear medicine, Quantification, Positron emission tomography, Metabolism, FDG, Brain.

Introduction

The brain is an organ with high metabolism but without an energy reserve (Catafau, 2001). Neuronal activity therefore depends on a continuous supply of oxygen and energy substrate, which is guaranteed by cerebral blood flow (CBF). The energy substrate is basically represented by glucose because fatty acids do not cross the blood-brain barrier, and energy generation from ketone bodies is only substantial during the first month of life of an animal (Nehlig, 1997). The intensity of cerebral activity is regionalized due to the organization of neuronal groups and the oxygen and glucose regulatory

and consumption mechanisms; thus, consumption is four times greater in the grey matter than in the white matter (Nehlig, 1997). The direct relationship between metabolism and CBF was initially postulated by Roy and Sherrington (1890) and is observed not only under physiological conditions but also in most diseases. Imaging techniques are applied for detecting cerebral blood flow or metabolism in a wide variety of clinical situations. Positron emission tomography (PET) and single-photon emission computed tomography (SPECT) are the main nuclear imaging modalities adopted, both of which provide functional information that is used in the diagnosis and prognosis of conditions such as epilepsy, dementia, brain neoplasms, and stroke (Blake et al., 2003; Silverman, 2004).

The first attempts to measure the metabolic rate of glucose used a ¹⁴C-labelled glucose molecule, [¹⁴C] glucose, which is metabolized via the same glycolytic pathway and the tissue concentration of which can be measured by autoradiography (Sokoloff et al., 1977). However, the disadvantage of [¹⁴C] glucose is the rapid rate at which it is converted to CO₂ and water. Because CO₂ is rapidly removed from tissues, the accumulation of radioactivity in the tissue is small and difficult to assess. Sokoloff and colleagues described the preparation

 This is an Open Access article distributed under the terms of the Creative Commons Attribution License, which permits unrestricted use, distribution, and reproduction in any medium, provided the original work is properly cited.

How to cite this article: Prando S, Ono CR, Robilotta CC, Sapienza MT. Methods for quantification of cerebral glycolytic metabolism using 2-deoxy-2-[¹⁸F]fluoroglucose in small animals. Res Biomed Eng. 2018; 34(3):254-272. DOI: 10.1590/2446-4740.04517

*Corresponding author: Hospital das Clínicas, Departamento de Radiologia, Serviço de Medicina Nuclear, Faculdade de Medicina, Universidade de São Paulo, Rua Dr. Ovídio Pires de Campos, 872, Cerqueira César, CEP 05403-911, São Paulo, SP, Brasil. E-mail: prando@usp.br

Received: 11 August 2017 / Accepted: 21 June 2018

of 2-deoxy-D- ^{14}C glucose (^{14}C -DG), a molecule that shares the metabolic pathway of glucose only at the steps of cellular internalization by the GLUT protein and phosphorylation by hexokinase. The generated product, 2-deoxyglucose-6-phosphate, does not undergo further metabolism and is retained inside cells, facilitating the measurement by autoradiography of the amount of glucose captured by the cells (Sokoloff et al., 1977).

Ido et al. (1978) published the results of the preparation of 2-deoxy-2- ^{18}F fluoroglucose (FDG), a DG molecule labelled with a positron emitter, fluorine-18, which allows obtaining images of glucose consumption using PET. This technique led to advances in the understanding of brain functioning and in the direct relationship between functional activity, metabolism and blood flow (Ingvar, 1982), as well as in the detection of tumours with high glucose uptake and metabolism. Although structurally different from DG, FDG is considered to be very similar to DG regarding its absorption and metabolism *in vivo* (Phelps et al., 1979; Sokoloff, 1981a; 1981b). Phelps et al. (1979) adopted the ^{14}C -DG model developed by Sokoloff (1977) to estimate the FDG kinetics and demonstrated that PET, with modelling for FDG, can be reliably used to estimate the rate of glucose metabolism.

Positron emission tomography is a well-accepted method for the quantitative and non-invasive imaging of biological functions; this technique enables physicians to monitor the presence of tracers labelled with positron emitters. The delivery, distribution, and kinetic patterns of a labelled compound in relation to the specific biomolecule in the target tissue are assumed to reflect specific biological functions in the living body.

The use of the same imaging techniques in pre-clinical studies of small animals (primarily rodents such as rats and mice) and clinical studies of humans presents the opportunity for direct translational research in drug discovery and development, the neuropharmacological basis of psychiatric disease, and the optimization of drug therapy (Hargreaves and Rabiner, 2014; Tsukada, 2012). Thus, PET studies in rodents can bridge the gap between pre-clinical and clinical research. However, the ideal pre-clinical animal model does not exist because enzyme systems and metabolism may differ between humans and other animals.

This work reviews the quantification methods of cerebral glycolytic metabolism most often applied in studies in small animals (i.e., rats and mice) using FDG as a radiotracer.

***Ex vivo* quantification methods: Autoradiography**

Histology and autoradiography are widely available techniques for anatomical and functional neuroimaging of small animals. Histological analysis is the gold

standard for an accurate description of neuroanatomy and the characterization of brain tissue. Autoradiography is a technique that allows visualization of molecules or fragments of molecules that have been radioactively labelled using X-ray film, phosphor imaging plates (IP), beta imaging systems, or photonuclear emulsion. Furthermore, this technique has been used for decades to quantify and localize drugs in tissues and cells (Solon, 2015).

Autoradiography is subdivided into two broad modalities commonly referred to as quantitative whole-body autoradiography (QWBA), or autoradioluminography, and microautoradiography (MARG). QWBA provides full-body, high-resolution images of the spatial distribution of radiolabelled compounds used in laboratory animals. The major advantages of QWBA include the possibility of determining compound concentrations in regions with thicknesses between 50 and 100 μm and minimal sample manipulation, thereby reducing the chance of cross-contamination and exsanguination effects that occur during tissue extraction. However, QWBA cannot provide data at the cellular level because the procedures necessary to freeze the sample alter the cellular morphology, which does not occur with MARG (Solon, 2015). MARG provides the possibility to visually localize radiolabelled compounds at the cellular level in a histological preparation, and it has been widely used to provide important information about cellular mechanisms.

Both techniques require that the animal be euthanized at a given time after the administration of the tracer. The carcass and the tissue (in the cases of QWBA and MARG, respectively) are frozen and cryosectioned to obtain representative samples of the tissue to be studied. The sections are dehydrated and exposed to IP along with radioactivity calibration standards. The resulting images are analysed to determine the concentrations and spatial distribution of the tracer in the tissue (Figure 1). Tissue tracer concentration versus time profiles can then be constructed to provide data for organ- or tissue-specific pharmacokinetic compartmental analyses, enabling the construction and examination of complete kinetic models of the entire body, specific tissues, or both.

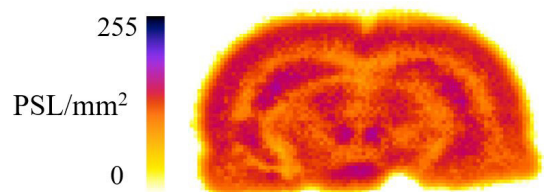


Figure 1. Coronal section of *ex vivo* autoradiography of the rat brain 1 h after intravenous injection of 37 MBq 2-deoxy-2- ^{18}F fluoroglucose; image plate resolution: 150 μm . PSL: photostimulated luminescence.

A multimodal approach for assessing the distribution of the radiocompound is often useful because QWBA can complement *in vivo* imaging strategies such as PET and SPECT, thereby providing images of the distribution of radioactivity in tissue with enhanced resolution. When the technique is performed with FDG and immediately after PET, certain considerations must be made. Generally, autoradiography experiments use C-14 or H-3, which have physical half-lives of years and require three or more days for the preparation of samples for sectioning and subsequent exposure. For these isotopes, thawing and dehydration steps are performed prior to IP exposure. In the case of FDG, the sectioned samples should be immediately positioned on the IP, and the cassette should be kept in a refrigerated environment to avoid resolution loss due to melting. Condensation should also be kept as low as possible to avoid water formation between the samples and the IP, which degrades image quality. Much of the signal that forms the image in the IP comes from the positrons, which have a short range. The IPs are relatively insensitive to high-energy gamma rays such as F-18; therefore, the sections should be positioned with the biological material facing the IP and with a minimum amount of material between them (Stout and Pastuskovas, 2011). To avoid contaminating the IP with the tracer, a thin plastic film can be used between them.

Both QWBA and MARG are based on exposing tissue samples containing radioactive material to radiographic films or stimulated phosphor plates (i.e., IPs). Radiological films have higher spatial resolution than IPs, while the latter are more sensitive. This characteristic allows for the reduction of the exposure time to 1/10 of that required for radiological film, a significant advantage when working with short half-life radionuclides. For quantification purposes, the use of IPs is also more advantageous because there is greater linearity between the radionuclide concentration and the image density information than that observed with radiographic film. The exposure time of the IPs depends on the radionuclide used, its physical half-life, decay mode and the expected amount of radioactivity present in the sample. Detailed information on IP calibration curves and resolution measures can be found in Knol et al. (2008) and Schmidt and Smith (2005).

To establish the relationship between the degree of uptake measured with the detection system and the metabolic rate, it is necessary to construct a calibration curve between known activity levels and the photosensitized luminescence per area resulting from the exposure. A calibration curve should be constructed for each experiment at the same time the IP is exposed to the radiation derived from the tissue studied. In addition, the user must estimate the transfer constants to obtain the total metabolic rate. After obtaining the preliminary

data, it is possible to calculate the absolute glucose consumption in different regions of the brain using specific software such as PMOD (www.pmod.com).

Although autoradiography is the gold standard for glucose metabolism quantification, it is important to note that autoradiography is for *ex vivo* use and, therefore, has little application in longitudinal studies. However, quantitative autoradiography data may be useful for making preliminary assessments or for determining whether PET studies are likely to have sufficient power for detecting specific regional changes in small animal images. In addition, high-resolution autoradiography is frequently used to validate the *in vivo* functional results obtained with equipment designed for small animals, and it remains a technical reference in research on functional brain images.

***In vivo* quantification methods: PET**

PET is based on the administration of molecules labelled with positron-emitting radionuclides, and the chemical form of the molecule is designed to investigate a process of interest, such as glucose uptake rates in the case of FDG. PET has evolved from an imaging mode based primarily on visual analysis into a fairly accurate quantitative imaging tool in which biological processes can be quantitated and compared in terms of binding potential or transfer rates. Factors that contributed to this evolution include the increased sensitivity and spatial resolution of the imaging systems (Sossi and Ruth, 2005).

New developments in PET equipment have improved the contrast and spatial resolution while maintaining a high sensitivity, but the spatial resolution is still a challenging problem, especially in relation to the intrinsic limit of the positron range before the particle is annihilated. The spatial resolution of PET in clinical studies is approximately 5-10 mm, while the resolution of a system for small animals with fluorine-18-labelled radiopharmaceuticals is 1-2 mm. Despite the lower absolute value compared to clinical studies, the spatial resolution of PET with FDG remains an important limiting factor in the evaluation of glucose metabolism in the brains of small animals because there is a worse ratio between the spatial resolution and the volumes of interest within anatomical structures (Byrnes et al., 2014).

Compared with humans, the activities of radionuclide injected into small animals are proportionally larger to maintain a signal-to-noise ratio close to that obtained in clinical images (Kung and Kung, 2005; Jagoda et al., 2004; van den Hoff, 2011). However, it is necessary to ensure that the tracer principle is not violated, i.e., that the mass of injected FDG stays at a concentration that does not interfere with the glucose metabolism and that no pharmacological effects occur.

A typical 37-MBq dose of FDG corresponds to a fraction of a nanogram of radioactive material. The specific activity is given as the ratio of the activity to the number of grams of material. In the case of FDG, this number is 349 MBq/ng, assuming that all of the FDG is radioactive. If stable FDG is present, there will be more grams of chemical FDG for the same amount of radioactive FDG. However, the total chemical quantity of FDG is insignificant from a pre-clinical point of view (Jadvar and Parker, 2005; Jagoda et al., 2004).

In addition to the resolution, the accuracy and precision of the quantifications in a PET study depend on time scales and, in some cases, the arterial input function.

The input function is the time function of the tracer concentration in the arterial blood or plasma that directly affects the rate of tracer transport in local tissue (Carson et al., 1993; Huang and Phelps, 1985). Several methods exist to obtain the input function; however, the manual collection of arterial blood is considered the gold standard in small animal research. Unfortunately, the manual collection has many drawbacks, including the need of a large number of blood samples, which may alter the circulation dynamics and lead to death due to blood loss or complicate longitudinal studies (Sijbesma et al., 2016). Moreover, sample manipulation increases the researcher exposure to radiation. In addition, the activity concentration of the samples should be measured with gamma counters calibrated for the radioisotope used with the PET device and corrected for radioisotope decay from the time of injection.

An alternative to manual arterial blood sampling is the use of automatic collection devices that measure the radioactivity of the β^+ concentration in the venous blood (Convert et al., 2007; Boellaard et al., 2001; Weber et al., 2002). However, additional corrections, such as for delay and signal dispersion, might be necessary to obtain an accurate input function (Munk et al., 2008; Senda et al., 1988). Moreover, a major drawback is the impossibility of analysing blood samples for radiometabolite-producing tracers to correct the input function. Fortunately, in FDG images, this is not required when the difference between the plasma and whole blood concentration is minimal, and the relationship between the two remains relatively constant over time (Zanotti-Fregonara et al., 2012).

Currently, much effort has been made to develop non-invasive techniques to obtain the input function. Image-derived input function (IDIF) is the most common approach. In this approach, a time-activity curve from the time of injection is drawn directly from the PET image using the amount of radioactivity emitted by large blood vessels or the left ventricle. Challenges, such as the temporal and spatial resolution of the device, intra-frame movement, and noise, as well as partial volume and spillover effects, make the application of

this technique a challenge for the brain imaging of small animals. In addition, the input function validated for a given device using certain acquisition and processing parameters cannot be used for another device without previous validation (Zanotti-Fregonara et al., 2011; Zanotti-Fregonara et al., 2009; Kim et al., 2006; Green et al., 1998).

Currently, another much exploited technique is the standardized arterial input function (SAIF). This technique assumes that the shape of the input function curve is constant among animals and that only the amplitude differs. Thus, the individual input function is obtained by averaging several arterial input functions purposely scaled to the individual characteristics of the animal using one or two blood samples. This technique has already been validated for humans and mice in FDG-PET images (Takikawa et al., 1993; Meyer et al., 2006). The main advantage is the absence of artefacts related to noise and partial volume because the technique does not require images to estimate the input function. However, two important restrictions exist: first, the tracer injection should be standardized for all animals; second, all animals should be metabolically similar (Zanotti-Fregonara et al., 2013; Meyer et al., 2017).

The choice of the best input function sampling method depends on the tracer kinetics and on the quantification method used. Quantification via compartmental model (CM) is primarily affected by the shape and occurrence time of the peak plasma concentration of the tracer, and small variations can lead to biased estimates of the micro- and macroparameters. Moreover, the application of non-invasive methods can lead to an increase in the uncertainty of the CM parameter estimates, which becomes a problem when groups of individuals are compared. Non-invasive input function sampling techniques have wide applicability using graphical methods because they are affected by neither the peak time nor the shape of the input function. Moreover, they primarily depend on the area under the curve, which is much easier to estimate than the input function (Zanotti-Fregonara et al., 2011; 2012).

Beyond the input function, the adequate standardization of image acquisition and processing, including factors such as the corrections applied to the acquired images and the chosen tomographic reconstruction and quantification techniques, is also important to improve the accuracy and precision of quantification (Frey et al., 2012; Vanhove et al., 2015).

In addition to these aforementioned technical factors, biological factors, such as the route of FDG administration (Vanhove et al., 2015; Schiffer et al., 2007; Fueger et al., 2006), dietary condition (Vanhove et al., 2015; Fueger et al., 2006), age of the animal (Nehlig, 1997), handling of the animal before and during the

FDG incorporation period (Vanhove et al., 2015), type of anaesthesia (Alstrup and Smith, 2013; Fueger et al., 2006), and glucose levels (Orzi et al., 1988; Viglianti et al., 2017) might alter the biodistribution of the compound. Intravenous administration is preferred due to the greater reproducibility, although intraperitoneal administration of the radiopharmaceutical is also possible (Schiffer et al., 2007). For PET imaging with the glucose analogue FDG, food is often withdrawn for hours before the experiment to reduce the plasma level of glucose, which competes with FDG for the uptake carrier (Vanhove et al., 2015). In rats, feeding is usually restricted for at least 12 h before the study (Deleye et al., 2014). As mice feed frequently and can reach a state of torpor after 7 h of food withdrawal, the fasting period should be kept at a minimum duration (Jensen et al., 2013). Animals kept in environments with very low room temperatures tend to produce heat through the metabolism of brown fat, which decreases the brain uptake of FDG. For this reason, it is recommended that the animal be kept on a heating plate throughout the entire preparation procedure and image acquisition.

There are several ways to acquire PET images. Acquisition can be performed in static, dynamic, or gated modes. For the quantification of cerebral physiological parameters such as blood flow, metabolism, or receptor concentration, static or dynamic images are used. Static acquisition refers specifically to the recording of the radiation emitted by the tracer present in the brain during a certain time interval within the study. The result is a single image that represents the average amount of radioactivity during the examination period. Only semiquantitative information can be derived from static acquisitions, the most well-known being the standardized uptake value (SUV; Huang and Wong, 2017). Dynamic images are composed of multiple sequential images so that the long-term behaviour of the tracer in the tissue can be observed. Dynamic acquisitions differ from a series of static images because they begin immediately after tracer injection, and the radioactivity from the tracer is monitored throughout the examination time and made available in the form of time-activity curves (TACs).

In dynamic images, the acquisition parameters such as the total examination time and the number and duration of the images acquired must be defined by the researcher. The total examination time primarily depends on two factors: the physical and biological half-lives of the tracer in the tissue of interest. Exams lasting a long period of time relative to the physical half-life do not improve the signal-to-noise ratio of the study. At the same time, the kinetics of the tracer, or its biological half-life, is also a determining factor of the total examination time. Tracers with faster kinetics provide biological information in a

brief period of time, reducing the total examination time (Huang and Wong, 2017).

Dynamic data are usually acquired when it is necessary to know the behaviour of the tracer in the system of interest, and it is the only way to obtain truly quantitative measures. Although the acquisition of dynamic images is slower, and the number of exams performed per day is reduced, its major advantage is the flexibility in formatting the data obtained, which produces dynamic images with different time intervals and even static images over a period of time determined by the researcher.

One problem in using the PET technique for *in vivo* studies of small animals is the need to contain the animals during image acquisition to avoid artefacts caused by movement. For this reason, animals should be physically restricted or anaesthetized. Because anaesthetics may cause significant changes in the physiology of the central nervous, cardiovascular and respiratory systems (Toyama et al., 2004), the measurement of FDG uptake in the brain can be compromised. Cerebral glucose consumption is typically reduced when the animal is anaesthetized, and FDG incorporation is reduced with most anaesthetic protocols, including inhalant anaesthetics (e.g., isoflurane or sevoflurane), ketamine, propofol, and pentobarbital (Alstrup and Smith, 2013; Matsumura et al., 2003). Because of the ease and speed with which the anaesthetic protocol can be changed, inhalant anaesthesia has been used in most small-animal imaging studies. Toyama et al. (2004) noted that, compared with animals that were kept awake during FDG incorporation, animals anaesthetized with isoflurane displayed a 29% decrease in brain uptake and a 91% increase in cardiac uptake. Ketamine, combined with the muscle relaxant xylazine, reduces brain and cardiac uptake by 39% and 64%, respectively. Xylazine directly stimulates the α_2 -adrenergic receptors of pancreatic islet cells causing the decrease in insulin release, thus, resulting in hyperglycaemia (Abdel el Motal and Sharp, 1985).

Because anaesthesia can cause respiratory depression and, in some cases, cardiovascular depression, these vital signs should be monitored. The animal should always be carefully monitored during the PET scanning because metabolic and physiologic changes, such as hypercapnia, hypoxia, hypothermia and acidosis, can influence the results. An alternative to reduce the effects of anaesthesia on brain metabolism is to keep the animal awake during the tracer incorporation phase and anaesthetise it only during image acquisition. Although this procedure is common in studies not intended to evaluate the effect of the anaesthesia on glucose metabolism, acquisition is limited to static images, and quantification techniques will be restricted to semiquantitative methods. Several research groups have developed methods that enable

the acquisition of dynamic images while the animal is conscious. Mizuma et al. (2010) developed a device that restricts animal movement during experiments to obtain time-activity curves throughout the tracer incorporation time. Although the animals receive training for acclimatization, stress cannot be excluded as a confounding factor in the results (Sung et al., 2009; McLaughlin et al., 2007).

Currently, several devices have been proposed that enable the acquisition of dynamic images without restricting the animal's mobility. The RatCAP is a miniaturized PET scanner surgically mounted directly on the animal's head (in the case of rats) that moves simultaneously with the animal to avoid movement artefacts (Vaska et al., 2004; Schulz et al., 2011). Although it is an interesting system that enables researchers to study the brain during periods of activation, the scanner has less sensitivity than commercial devices, and can inhibit animal movement and cause stress. The most modern system used currently is motion compensation (Spangler-Bickell et al., 2016; Kyme et al., 2011; Weisenberger et al., 2005). In this method, the awakened animal is confined to a small space during image acquisition, and its head movement is measured and subsequently corrected so that the image can be reconstructed without movement artefacts. Of all of the methods in use, this is the one that causes less stress during examination.

Crone (1965) showed that glucose transport in the brain is affected by the plasma glucose concentration and that transport was performed by two mechanisms: passive and facilitated diffusion. Several studies have reported that FDG absorption by the cerebral cortex keeps an inverse relationship with blood glucose levels (Viglianti et al., 2017; Alf et al., 2013; Claeys et al., 2010). Orzi et al. (1988) reported that hyperglycaemia causes a competitive inhibition of FDG incorporation. However, the nonlinear response to increased glucose and the change in the cerebral FDG uptake pattern of patients with moderate hyperglycaemia observed by Viglianti et al. (2017) and Kawasaki et al. (2008) suggest that the FDG uptake mechanism is more complicated than as proposed by Crone (1965), and that it cannot be explained only on the basis of substrate competition. Under normal conditions, GLUT1 functions at less than its maximum capacity, thus, it is not a rate-limiting factor for brain function (Leybaert et al., 2007). In contrast to glucose transport, glucose phosphorylation via hexokinase is the rate-limiting step for brain energy metabolism in a hyperglycaemic state (Cunnane et al., 2011). In a clinical study, Viglianti et al. (2017) suggested that the lumped constant, which represents the correction factor for the differences in glucose and DG transport and phosphorylation rates, is not uniform over the physiological range under which imaging generally

occurs, given the nonlinear relationship between plasma glucose and whole brain SUV. The change in lumped constant with plasma glucose has been observed in previous studies of small animals (Schuier et al., 1990; Suda et al., 1990), and this variation is likely caused by a change in the distribution volume due to the changes in transport and metabolism under hyperglycaemic conditions (Crane et al., 1983).

FDG-PET-based methods for analysing glucose uptake by cells can be divided into qualitative, semiquantitative and quantitative methods. Qualitative methods are purely visual and exhibit greater variability among investigators with different degrees of training, and are not the object of this review. Semiquantitative and quantitative methods, such as SUV and compartmental models, are presented below. Other methods, such as spectral analysis (Veronese et al., 2016; Cunningham and Jones, 1993) and kinetic modelling in the projection space (Germino et al., 2017; Wang and Qi, 2013), are also used in preclinical studies. However, they will not be covered in this article. Although the voxel-based analysis is not a quantification method, but can be used only for comparison, it will be addressed in this review because of its relevance in clinical and preclinical research.

Semiquantitative methods

Standardized uptake value (SUV)

Among semiquantitative methods, the most well-known is SUV, which relates tissue activity to the injected activity and the individual's body weight or area. The SUV or, alternatively, the maximum SUV in a volume of interest (SUV_{max}), has been used in many studies and been found to be useful as a benchmark in clinical studies.

The SUV is a parameter that characterizes the relative concentration of the radiotracer in the volume of interest, and is often used as a piece of data complementary to the visual evaluation of an image. To obtain SUV, careful standardization of the method and recording of the injected radioactivity levels, animal weight and injection time are necessary, as reproducibility is limited when different acquisition and processing protocols or equipment are used (Sapienza and Buchpiguel, 2017). The calculation is simple and can be expressed in equation 1:

$$SUV = \frac{C_{PET}(t)}{(Injected\ activity / Patient\ weight)} \quad (1)$$

where $C_{PET}(t)$ represents the concentration of FDG in the region of interest (ROI) in a specific time.

Therefore, a SUV of 1 indicates that the counts obtained in the volume of interest are equal to the value expected if the activity were homogeneously distributed in the animal. However, the SUV may be affected by

multiple factors, from physiological changes between or within individuals to technical factors related to acquisition, processing or quantification (Köroğlu et al., 2017). Among the technical issues, image noise and the ROI segmentation method affect the SUV, and may produce biased results (Boellaard et al., 2004; Krak et al., 2005; Tyłski et al., 2010; Silva-Rodríguez et al., 2015). Many segmentation techniques have been described with the objective of reducing intra- and inter-observer inconsistencies (White et al., 1999). Image segmentation methods can be divided into three groups based on the degree of human involvement: manual segmentation, semi-automatic segmentation, and fully automatic segmentation (Karsch et al., 2009; Fasihi and Mikhael, 2016). The technique most used currently in PET for segmentation is the manual technique followed by the semiautomatic one. Silva-Rodríguez et al. (2015) conducted a study based on simulated PET images with FDG to compare the effects of the activity and ROI used to calculate the SUV. The SUV_{50} , obtained by applying a threshold of 50% of the maximum value, and the SUV_{mean} showed the best performance in regard to accuracy and repeatability, respectively. Another important factor to note is the variation in SUV with the FDG activity used. The SUV_{mean} and SUV_{50} were less affected than the SUV_{max} by the reduction in injected activity, i.e., by increase in noise (Silva-Rodríguez et al., 2015).

In clinical studies, the SUV_{max} is used more widely than the SUV_{mean} because it represents the voxel with the highest uptake and presumably the area with the highest metabolic rate in the analysed volume. However, in studies with small animals, the SUV_{mean} (Figure 2) is more commonly used because this parameter is less susceptible than the SUV_{max} to statistical fluctuations in counts.

The SUV is often used as a substitute for the glucose uptake rate (K_i) or absolute glucose uptake

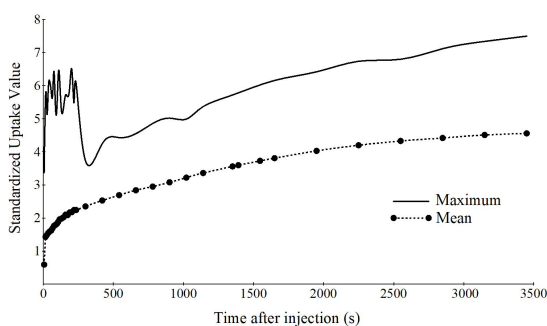


Figure 2. Mean and maximum standardized uptake values curves of rat brain, measured for approximately 1 h after intravenous injection of 37 MBq 2-deoxy-2-[^{18}F]fluoroglucose. Activities were measured within a region of interest over the whole brain. The positron emission tomography list-mode data were separated into 36 frames (1x5, 11x10, 1x12.5, 7x15, 1x67.5, 7x120, 1 x 210, 7x300 sec).

(MRGlu) (Durand and Besson, 2015). However, its accuracy depends on two factors: the amount of unmetabolized FDG present in the ROI used in the quantification and the condition that the activity normalized by weight, lean mass, or body surface area is proportional to the integral of the FDG concentration during the study time (Kotasidis et al., 2014).

In quantification via SUV estimation, the selected ROI contains information on the metabolized and unmetabolized FDG concentrations present both in the vascular and extravascular compartments. When the ROI has FDG metabolism rate close to that of the surrounding tissues, its assessment using the SUV is particularly hampered by the presence of free FDG in the vascular and/or intracellular compartment (Allen-Auerbach and Weber, 2009). In such cases, the SUV contrast between the ROI and the background is diminished by the inclusion of unmetabolized FDG, which can be treated as a “biological noise”, which is a problem, especially in cases of post-therapeutic assessment, where the FDG concentrations in the tissues surrounding the lesion may be substantially larger, causing problems in the interpretation of results (Sugawara et al., 1999). Efforts have been made to estimate the amount of metabolized FDG in tissues, such as the liver and spleen (Keramida et al., 2017). In FDG studies, SUV also can be corrected for plasma glucose level, because glucose transporters may be saturated by glucose. SUV is multiplied by plasma glucose concentration and normalized by normal blood glucose level of 5.55 mmol/L (100 mg/dL). The normalisation of glucose level may decrease variability and increase the degree of concordance between studies in cases of high plasma glucose variability and the presence of extreme blood glucose values in the population studied (Paquet et al., 2004).

In addition to the amount of unmetabolized FDG, the SUV method considers that the metabolism is related to the total body weight (BW), lean body mass (LBM), or body surface area (BSA) of the animal. The BW has been used most commonly in normalization for the calculation of the SUV, regardless of whether the study is conducted with small animals or humans. However, changes in body weight or composition, which often occur in cancer patients resulting from the disease or treatments, can change the FDG distribution and dynamics in plasma, moving away from the value of the integral of activity normalized by BW, LBM or BSA (Huang, 2000). The differences between these values make unreliable the substitution of the kinetic parameters (K_i and MRGlu) by the SUV (Durand and Besson, 2015; Weber et al., 1999). To minimize the problem of correlation between the plasma FDG dynamics and the normalization applied to the SUV, more robust quantification methods using blood samples obtained during the exam time, also

known as input functions, should be used (Ishizu et al., 1994; Thie, 1995).

In addition to the problems mentioned above, disadvantages of this method include its poor reproducibility, which is closely related to maintaining the acquisition and processing parameters of study constant, the non-extravasation at the injection site, and the definition of the area/volume of interest, which is a challenge in small animal imaging (Adams et al., 2010).

Quantitative methods

More detailed information on glucose metabolism can be obtained through quantitative methods, as described in Strauss et al. (2011). Of these, the most best accepted are compartmental analysis and graphical analysis, according to Patlak et al. (1983) and Patlak and Blasberg (1985).

Absolute quantification using the Compartmental Model (CM)

CM, also known as the kinetic model, is the most accurate method of PET data analysis. Gunn et al. (2001) have provided an overview and comprehensive analysis of the mathematics underlying the CM in PET. In the CM applied to PET (Figure 3), we assume that FDG is exchanged between compartments, with each compartment representing a homogeneous physiological or biochemical entity, and the rates at which the radiotracer is transferred between the compartments are described by first order differential equations.

In the CM, FDG is transported from plasma into tissue as free FDG and is subsequently metabolized into FDG-6-PO₄. The concentrations of FDG in the compartments are those of free FDG in plasma (C^{*}_p)

and in tissue (C^{*}_T), and the concentration of metabolized FDG (C^{*}_m). The microconstants for the transfer of FDG, K^{*}₁ (μmol/min/100g) and k^{*}₂ (min⁻¹), represent the transport, mediated by the transporters of glucose across the cell membrane. The constants k^{*}₃ (min⁻¹) and k^{*}₄ (min⁻¹) represent the phosphorylation of FDG by hexokinase and dephosphorylation by glucose-6-phosphatase, respectively.

The CM requires dynamic imaging from the moment of injection and, in general, arterial blood samples to measure the plasma radiotracer concentration as a function of time, defined as the input function. Because the CM estimates kinetic parameters, we can determine glucose transport and hexokinase activity for each ROI in the image.

We can estimate the microconstants for glucose using the equations 2 and 3 (Fang and Muzic, 2008):

$$\frac{dC_p(t)}{dt} = K_1 C_p(t) - (k_2 + k_3) C_T(t) + k_4 C_m(t) \tag{2}$$

$$\frac{dC_m(t)}{dt} = k_3 C_T(t) - k_4 C_m(t) \tag{3}$$

Solving the differential equations above allows expressing the free glucose concentration in the tissue (C_T) in terms of the plasma concentration (C_p), and the rate of glucose metabolism (MRGlu) in terms of C_p is thus obtained by the equation 4:

$$MRGlu = \phi k_3 C_T = \frac{K_1 k_3 \phi}{k_2 + \phi k_3} C_p \tag{4}$$

The difficulty in using the equation above is that the values of the transfer rates for glucose (K₁, k₂ and k₃) must be determined. The direct measurement of these

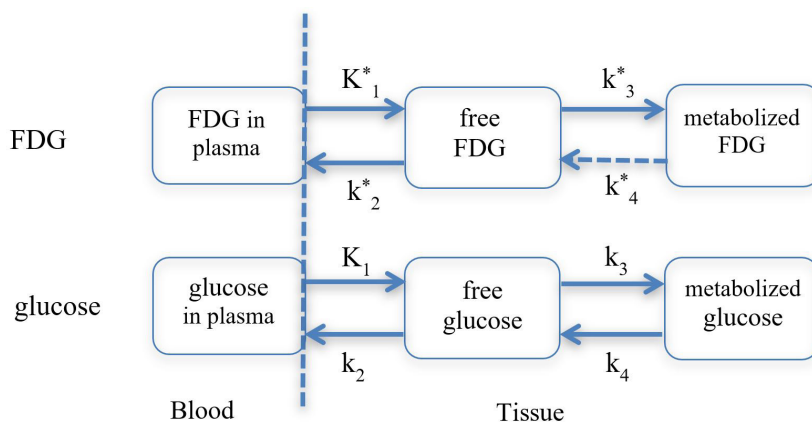


Figure 3. Two-compartment model depicting the transport of glucose and 2-deoxy-2-[¹⁸F]fluoroglucose (FDG) to and from plasma to tissue, showing the rates of transport of the tracer/glucose into (K^{*}₁, K₁) and out of the cells (k^{*}₂, k₂), as well as the rates at which these molecules are converted to a form that is unable to leave the cell (k^{*}₃, k₃) and conversion from the trapped form back into the membrane-permeant form (k^{*}₄, k₄). In brain studies with FDG, it is often assumed that the dephosphorylation rate of FDG-6-phosphate in the brain tissue is small enough to be ignored (k^{*}₄ = 0).

transfer rates is too complicated; therefore, measurements of the PET TAC are used to estimate these values for FDG. The constant Φ represents the fraction of the phosphorylated glucose that is further metabolized in the glycolytic pathway. Sokoloff (1981a) demonstrated that in brain tissue Φ is very close to 1, indicating that only a small portion of the phosphorylated glucose will be dephosphorylated. For this reason, k_4^* can be considered negligible.

Through the use of the lumped constant (LC) adjustment term (Sokoloff et al., 1977; Moore et al., 2000; Krohn et al., 2007), which represents the correction factor for the differences in glucose and DG transport and phosphorylation rates, and allows converting the results obtained using DG to glucose. In the brain, DG is transported 1.4 times faster than glucose, while glucose is metabolized 2.5-4.5 times faster than DG (Dienel, 2012), thereby the rate of glucose metabolism can be expressed as in equation 5:

$$MRGlu = \frac{K_1^* k_3^* C_p}{k_2^* + k_3^* LC} = K_i^* \frac{C_p}{LC} \tag{5}$$

Thus, MRGlu can be estimated with a simple equation from only the constant rates of FDG (K_1^* , k_2^* and k_3^*), the steady state C_p and LC.

In the LC, the distribution volume is the component sensitive to the glucose concentration due to the higher metabolism/transport rate of glucose in relation to DG. Under physiological conditions, where blood glucose remains constant, LC remains relatively stable. However, under conditions that include factors that alter plasma glucose concentration and consequently result in changes of greater or lesser magnitude in LC, LC should be determined for the specific conditions of the study. Several studies have shown changes in LC in hyperglycaemic (Orzi et al., 1988; Schuier et al., 1990), hypoglycaemic (Suda et al., 1990) and anaesthetized (Alf et al., 2014) animals, or in animals with tumours (Spence et al., 1998).

The model provides detailed information regarding glucose transport and metabolism as shown in Figure 4.

The advantages of this method are its reliability and its independence from examination or plasma clearance time, in contrast to the SUV. An important technical difficulty is the need for arterial cannulation to draw blood for the input function. It is also necessary to ensure injection without extravasation, which can be standardized using intravenous cannulation and an infusion pump. Another critical factor for the execution of this technique is the synchronization between the sampling times of arterial blood and PET imaging, since these data will be used in the differential equations shown above.

Patlak graphical analysis

Graphical methods allow the appropriate estimation of certain combinations of microparameters by transforming the estimation equations on which the CMs are based. The best-known graphical method for irreversible substances is the Patlak method (Patlak et al., 1983; Patlak and Blasberg, 1985). This method is a linearization of the compartmental equations for irreversible tracers (Figure 5). It can be shown that at a certain time t^* after the beginning of the tracer injection, all reversible compartments must be in steady state, i.e., the tracer concentrations in the plasma and in reversible tissue compartments should remain stable. This time depends on the tracer, the subject and the ROI. The relationship between the TAC of the tissue $C_T^*(t)$ and the TAC of the plasma $C_p^*(t)$ (y-axis) and the ratio between the integral and the instantaneous value

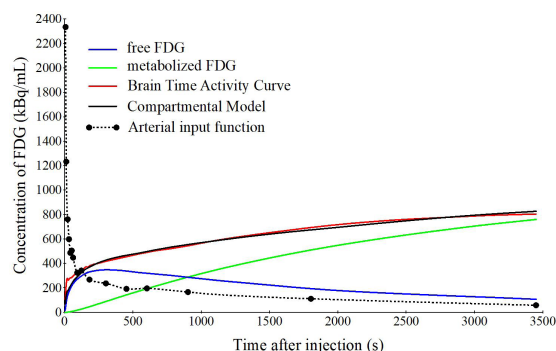


Figure 4. Compartmental model of 2-deoxy-2-[¹⁸F] fluoroglucose metabolism based on the radiotracer concentration curves as a function of time in the arterial input function (plasma) and volume studied (brain), illustrating the concentration of free and metabolized FDG estimated for approximately 1 h after the intravenous injection of 37 MBq FDG.

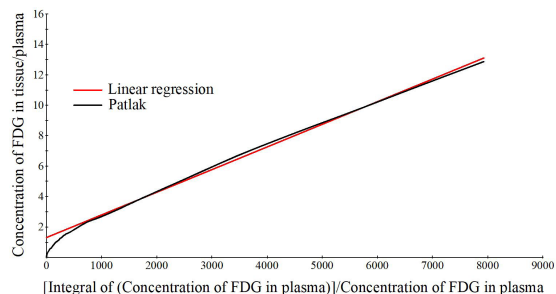


Figure 5. Patlak plot generated from the input function (plasma) and time activity curve from the brain in a representative animal after the intravenous injection of 37 MBq of 2-deoxy-2-[¹⁸F] fluoroglucose. The Patlak plot becomes linear after the tracer concentrations in reversible compartments and in plasma are in steady state. The slope of the linear phase of the plot is the net uptake (influx) rate constant K_i .

of $C_p^*(t)$ (x-axis) becomes linear at time t^* ; that is, the system reaches a steady state, expressed by equation 6:

$$\frac{C_T^*(t)}{C_P^*(t)} = K_i^* \frac{\int_0^t C_P^*(u) du}{C_P^*(t)} + V \quad (6)$$

K_i^* indicates the rate at which the tracer is irreversibly retained and can be calculated from the equation 6 using a simple linear estimation procedure.

This method requires the acquisition of dynamic images, beginning 15 to 30 min after the tracer injection, as well as arterial blood samples. Due to the linearity of the above equation 6, this method is much faster and less sensitive to noise, and therefore suitable for voxel-level applications. For FDG, we can calculate the MRGlu ($\mu\text{mol}/\text{min}/100\text{g}$) from K_i^* using the equation 7:

$$MRGlu = K_i^* \frac{C_p}{LC} \quad (7)$$

Although this approach enables an operational simplification of the CM, the disadvantage of the Patlak method is the inability to calculate the kinetic parameters separately; for FDG, for example, the method does not discriminate between glucose transport and hexokinase activity.

To determine the best quantitative method, one can examine whether there is need to estimate glucose transfer constants or only the amount of glucose metabolized is sufficient to characterize the change studied. Several criteria exist for kinetic model preference identification for brain PET studies. The most commonly used models are Akaike Information Criterion (AIC), AIC unbiased, model selection criterion (MSC), Schwartz Criterion (SC) and F-test. However, all model selection criteria resulted in similar conclusions for PET FDG (Golla et al., 2017).

Voxel-based analysis (VBA)

Prior to the advent of VBA, PET brain images were manually analysed via manual delineation of ROIs to investigate the existence of areas with altered metabolism. This approach was established for autoradiograph analyses of basic neurophysiological and metabolic scans of humans (Friston, 2007). In addition to being time consuming, the ROI method might introduce inaccuracies into the analysis because it is an evaluator-dependent. However, the most significant difficulty is that ROI analyses are usually guided by *a priori* information of the change in a certain brain region; therefore, possibly significant effects outside the specific ROI can be lost or the treatment/intervention can induce a global effect that is expressed in all ROIs. To overcome the challenge of detecting regional changes when a global change is present, the Statistical Parametric Mapping (SPM) software was developed (Wellcome Department of

Cognitive Neurology, Institute of Neurology, London, UK; Friston et al., 1994). SPM is the best-known VBA method that can be applied on a large scale in brain studies of humans and animal models of different neurological diseases or behaviours (Litaudon et al., 2017; Park et al., 2017; Cui et al., 2015; Casteels et al., 2010; Frumberg et al., 2007). SPM uses statistics to identify regions with different perfusion or metabolic rates or different volumes present in images obtained by SPECT, PET, or magnetic resonance imaging (MRI).

The SPM analysis method is based on the spatial representation of the parameters obtained (e.g., perfusion, metabolism, or volumes) via a VBA comparison of an animal (or group of animals) with a reference group of animals of the same species subjected to the same image modality. Before performing an SPM analysis, the images must be processed. This processing step is composed of three parts: spatial realignment, spatial normalization, and filtering. After this step, statistical analysis, intensity normalization and inference are performed. The most significant differences between groups are presented as a table of coordinates to represent three outline views of the brain (i.e., the glass brain) or as patches of colour on an MRI brain "slice", with the colours that represent the location of the voxels that have shown significant differences (Figure 6).

Spatial realignment, also known as the rigid registration method, involves correcting the difference in the position between the different acquired images due to differences in the positioning of the animals, through an inelastic transformation of the images.

Spatial normalization is performed to eliminate individual differences and ensure the positioning of the image voxels, so that the same structure occupies the same coordinates in all of the images. This normalization involves a stereotactic transformation of the brain images to fit an external anatomical model, the template, which corresponds to an atlas of standard anatomical space. The established and most commonly used atlases of the mouse and rat brain (Paxinos and Watson, 2017; Swanson, 2004) provide a series of sections, cut at specified angles, with external surfaces and internal boundaries of areas and nuclei indicated, as well as names assigned to the delineated structures. Atlases with 3-D representations of major brain structures have also been developed for the mouse (Chan et al., 2007; Gustafson et al., 2004; Lein et al., 2007; MacKenzie-Graham et al., 2004). This procedure allows direct intra- and inter-subject comparisons and the application of standard reference maps and masks.

Because of the relatively large differences in the spatial resolution between MRI and FDG-PET images of small animals, the automated image realignment of FDG-PET data with MRI templates is difficult primarily because

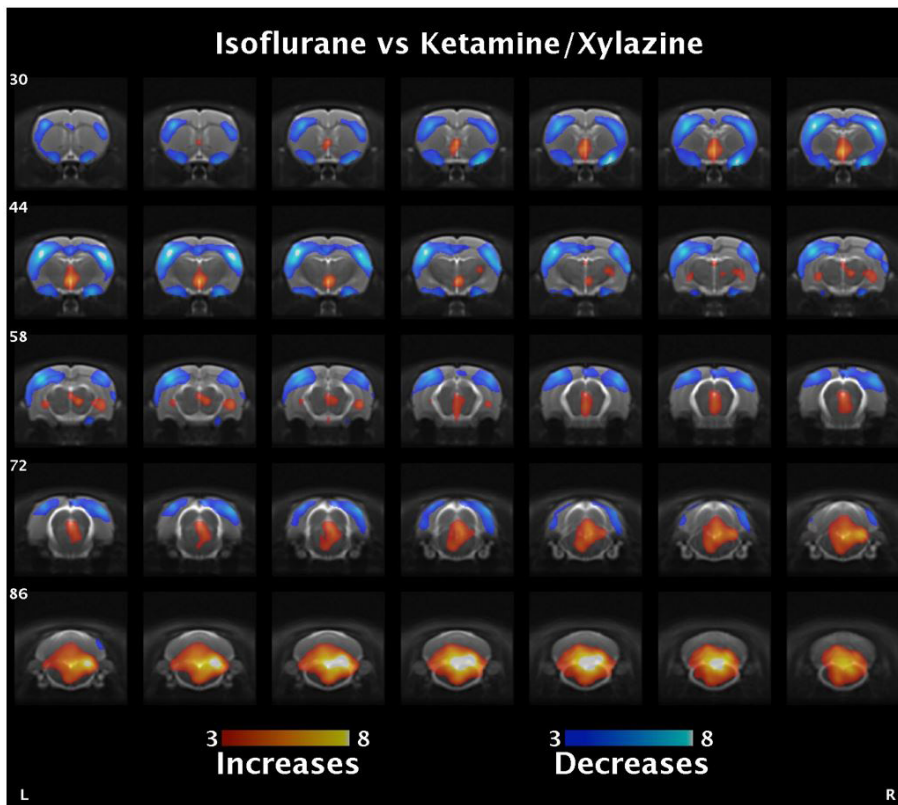


Figure 6. Representative rat brain images obtained by statistical parametric mapping of the standardized uptake values to compare rats kept under isoflurane and ketamine/xylazine anaesthesia during the 2-deoxy-2- ^{18}F fluoroglucose uptake period. T-map data (visualization cut-off point: $p < 0.05$; uncorrected) are depicted using Mango as a multi-slice coronal of magnetic resonance imaging template overlay (Schwarz et al., 2006). The colour bar was set to a minimum of 3 and a maximum of 8 for both increases and decreases in glucose uptake for isoflurane anaesthetised subjects ($n=15$) compared with ketamine/xylazine anaesthetised subjects ($n=18$).

of differences in the biodistribution of the tracer and the number of anatomical landmarks (Nie et al., 2014). Therefore, the availability of specific tracer templates aligned in a standard reference space enables the use of the automatic normalization of functional images, which minimizes user-dependent variability and provides direct access to the corresponding anatomical atlases and reference coordinates. Several standard anatomical and functional space models have been developed and tested for the spatial normalisation of small rodent brains (Poussier et al., 2017; Vallez Garcia et al., 2015; Nie et al., 2014; 2013; Coelho et al., 2011; Casteels et al., 2006; Schweinhardt et al., 2003).

After the normalization step, the images are smoothed by applying a spatial filter. The main objective of spatial filtering is to eliminate residual noise and allow the application of the random Gaussian field (RGF) theory. In practice, the intensity value of a voxel is replaced by the weighted average density of the neighbouring voxels, which increases the signal-to-noise ratio and adjusts the anatomical and functional variations between subjects (Friston, 2002). According to matched filter theorem,

the optimum smoothing kernel corresponds to the size of the anticipated effect. Thus, the optimum smoothing level is related to the size of the signal to be detected (Reimold et al., 2006). Unfortunately, the effect size is unknown most of the time and may undergo variations across brain studies. Welch (2013) tested various smoothing levels (0-1.5 mm) in mouse brain FDG-PET images. Although the sensitivity of the test was not significantly altered by different smoothing levels, the T-score increased between 5 and 15%. In addition to increasing the signal-to-noise ratio, spatial filtering causes the errors to approach the normal distribution, which ensures the validity of the inferences based on parametric tests.

Importantly, spatial smoothing has disadvantages in small animal brain studies. Spatial smoothing always decreases spatial resolution; therefore, the detection of small structures can be attenuated below the cut-off value attributed in the study. Therefore, it is critical to assess whether the objective of the study is accurate spatial localization because the technique might not identify small structures with low uptake. In this case,

autoradiography can be used to perform a preliminary evaluation of the structures and regional metabolic changes involved in the study.

The mean level of brain metabolism varies among different subjects and, to a lesser degree, in the same subject over time. To perform longitudinal or transverse comparisons of metabolism between subjects, it is necessary to adjust the intensity data. There are several techniques to adjust the average metabolic differences between subjects. However, the easiest way to correct these fluctuations is the count normalization to the cerebral global mean, so-called global normalization. The cerebral global mean is determined automatically by SPM as the mean voxel value of those exceeding a threshold (Buchert et al., 2005), and is implemented as default in the count-scaling algorithm, thus enabling to adjust for interindividual variability without the need of additional analyses. For this reason, global normalization by means of proportional scaling or analysis of covariance (ANCOVA) has found a wide utilization in SPM analyses of FDG brain PET data. In proportional scaling, it is considered that the subjects have an identical metabolic level, and to reach it is scale each scan by its estimated global activity (Gispert et al., 2003). This approach is based on the assumption that the measurement process introduces a global scaling of image intensities at each voxel, a gain factor. Another approach, ANCOVA, is to include the mean corrected global activity as an additional regressor in the model. Data with lower variance may be normalised by ANCOVA, while those with higher variance and number of subjects are better normalised by proportional scaling (Gispert et al., 2003).

The main problem with these intensity normalisation techniques is that they do not contemplate the possibility that the studied effects could modify the mean values of metabolism. As a consequence, the impact of regional influences on the general metabolism is lost, or areas with apparent hypermetabolism are created, as in SPM analysis of Alzheimer disease (Yakushev et al., 2009). To avoid this type of problem, we can normalise the images by ROI or cluster-based normalization, which includes only areas not affected by the pathology/intervention. In these cases, it is possible to use the average or maximum value. In the case of the mean value, it is necessary to choose an area in which the mean value is similar in all individuals. Of course, one of the precepts of the technique is to know which regions are not affected. Instead of using the mean value of the parameter of interest (SUV, MRGlu, Ki, among others) in these regions, one may use the maximum value because there is a significant probability that regions with higher metabolic rate are not affected by the pathology/intervention that decreases the consumption of glucose (Gispert et al., 2003).

Several of these techniques have been applied in studies of neurological diseases (Dukart et al., 2013; 2010; Yakushev et al., 2009). The choice of the best normalisation method for a given study can be based on the coefficient of variation of noise analysis (Gispert et al., 2003).

The disadvantage of VBA is the need to acquire multiple images from the same animal or from different animals to perform the comparison. Several possible comparisons are used in VBA and depend on the experimental design employed. In longitudinal studies, it is possible, for example, to compare the same animal at different times using a paired t-test. In transversal studies, it is possible to compare an individual against a group or to compare different groups submitted to different interventions. In many research projects, a bank of images from healthy animals must be built for comparison. However, for the interpretation of changes between groups, only the clusters should be compared as to avoid false positive results due to noise present in the voxels (Vállez Garcia et al., 2015). The size of the cluster must be defined according to the data acquisition and processing conditions (spatial resolution, voxel size).

Numerous parameters obtained with quantitative methods can be compared between groups using the VBA method, such as absolute glucose uptake, transfer rate constants, SUV and blood.

Discussion and conclusions

The major practical differences between the application of the quantification methods for humans and those used for small animals are related to spatial resolution, time scale, and arterial input function (van den Hoff, 2011). Many target structures of small animal PET are not much larger than the spatial resolution limit, and the limited recovery of true signal intensity frequently plays a much larger role in these conditions compared with human PET. In the case of small animals, the incomplete recovery of the signal directly translates into a corresponding reduction of the absorption parameters obtained, as K_1 and, indirectly, the SUV. Regarding the structures with dimensions close to the spatial resolution limit of the tomograph, the incomplete recovery of the signal must be corrected, which in turn requires a precise knowledge of the size and shape of the object.

Although not mandatory for all quantification methods, the arterial input function is limited by practical considerations. The most important factor to consider is the blood volume of rats and (especially) mice, which are frequently used in FDG studies. The removal of a relatively small volume of blood may result in physiological changes, which can cause significant changes in the quantification results. Other factors related to the

Table 1. Advantages and disadvantages of methods to analyse cerebral glucose metabolism with 2-deoxy-2-[¹⁸F]fluoroglucose.

Method	Advantages	Disadvantages
Qualitative (visual)	<ul style="list-style-type: none"> - Non-invasive. - Relatively fast. 	<ul style="list-style-type: none"> - Depends on the interval between injection and image acquisition. - Subjective.
Standardized uptake value	<ul style="list-style-type: none"> - Semi quantitative. - Good reproducibility if acquisition and processing are standardized. - Can be applied to static or dynamic images. 	<ul style="list-style-type: none"> - Depends on the interval between injection and image acquisition. - Does not provide constants rate or free and metabolized FDG concentrations.
Voxel-based analysis	<ul style="list-style-type: none"> - Comparative. - Good reproducibility. - Allows evaluating the whole brain. - Can be applied to static or dynamic images. 	<ul style="list-style-type: none"> - Requires a reference group/bank of normal subjects. - Not adequate for small clusters.
Patlak	<ul style="list-style-type: none"> - Quantitative. - Possibility of obtaining parametric image of K_{ir}^*. - Start of image acquisition after 20 min of injection. 	<ul style="list-style-type: none"> - Acquisition of dynamic image and input function. - Does not provide rate constants (K_{1r}^*, k_2^* and k_3^*). - Quantification based on predefined ROIs.
Compartmental model	<ul style="list-style-type: none"> - Quantitative. - Allows evaluating rate constants. - Possibility to obtain parametric images of K_{1r}^*, K_{1p}^*, k_2^*, k_3^*. 	<ul style="list-style-type: none"> - Acquisition of dynamic image and input function. - Noise in the initial images. - Necessity of synchronization between the start of image acquisition, injection and input function.
Autoradiography	<ul style="list-style-type: none"> - Quantitative. - High spatial resolution. - Can be performed with the same dose and immediately after PET-FDG. 	<ul style="list-style-type: none"> - <i>Ex vivo</i>. - Provides a planar image. - Not possible to perform longitudinal studies in the same animal.

PET: positron emission tomography; ROI: region of interest.

animal, the acquisition and processing technique should be standardised and controlled during the experiment.

Some advantages and disadvantages of the available quantification methods (Table 1) should be weighed according to the objective of the study. In the context of preclinical research, semiquantitative and quantitative methods are preferred because these approaches provide objective analysis parameters that are not dependent on expertise in visual analysis of images. VBA has a significant advantage over the SUV, since it allows analysis of the whole brain without the *a priori* formulation of a hypothesis. In addition, statistical methods, such as SPM, reveal regional differences in metabolism that are not always visually detectable.

Quantitative methods, while providing more reliable results, however, there are several technical challenges associated with these methods. Besides that, professionals with specific skills also are required to perform image acquisition and processing. Many factors can influence the results obtained; fortunately, these influences can be studied and minimized via the appropriate standardization of the acquisition, processing, and data analysis steps.

Although autoradiography is the gold standard for quantification, this method is not widely used in research protocols because it is an *ex vivo* method and does not allow longitudinal studies. However, autoradiography

can be used to verify the changes visualized by other quantification methods.

In conclusion, analysis and interpretation of PET data are not always simple, and the results will depend on many details in the study. Several approaches are available for the quantification of PET data, and the integration of data from multiple methods can strengthen the validity of the results obtained and enable the researcher to understand the problem from different perspectives.

References

- Abdel el Motal SM, Sharp GW. Inhibition of glucose-induced insulin release by xylazine. *Endocrinology*. 1985; 116(6):2337-40. <http://dx.doi.org/10.1210/endo-116-6-2337>. PMID:2986946.
- Adams MC, Turkington TG, Wilson JM, Wong TZ. A systematic review of the factors affecting accuracy of measurements. *AJR Am J Roentgenol*. 2010; 195(2):310-20. <http://dx.doi.org/10.2214/AJR.10.4923>. PMID:20651185.
- Alf MF, Duarte J, Lei H, Krämer S, Mlynarik V, Schibli R, Gruetter R. MRS glucose mapping and PET joining forces: re-evaluation of the lumped constant in the rat brain under isoflurane anaesthesia. *J Neurochem*. 2014; 129(4):672-82. <http://dx.doi.org/10.1111/jnc.12667>. PMID:24471521.
- Alf MF, Duarte J, Schibli R, Gruetter R, Krämer S. Brain glucose transport and phosphorylation under acute insulin-induced hypoglycemia in mice: an 18F-FDG PET study. *J Nucl Med*. 2013; 54(12):2153-60. <http://dx.doi.org/10.2967/jnumed.113.122812>. PMID:24159048.

- Allen-Auerbach M, Weber WA. Measuring response with FDG-PET: methodological aspects. *Oncologist*. 2009; 14(4):369-77. <http://dx.doi.org/10.1634/theoncologist.2008-0119>. PMID:19357228.
- Alstrup AK, Smith D. Anaesthesia for positron emission tomography scanning of animals brains. *Lab Anim*. 2013; 47(1):12-8. <http://dx.doi.org/10.1258/la.2012.011173>. PMID:23349451.
- Blake P, Johnson B, VanMeter J. Positron emission tomography (PET) and single photon emission computed tomography (SPECT): clinical applications. *J Neuroophthalmol*. 2003; 23(1):34-41. <http://dx.doi.org/10.1097/00041327-200303000-00009>. PMID:12616088.
- Boellaard R, Krak N, Hoekstra O, Lammertsma A. Effects of noise, image resolution, and ROI definition on the accuracy of standard uptake value: a simulation study. *J Nucl Med*. 2004; 45(9):1519-27. PMID:15347719.
- Boellaard R, van Lingen A, van Balen SC, Hoving BG, Lammertsma AA. Characteristics of a new fully programmable blood-sampling device for monitoring blood radioactivity during PET. *Eur J Nucl Med*. 2001; 28(1):81-9. <http://dx.doi.org/10.1007/s002590000405>. PMID:11202456.
- Buchert R, Wilke F, Chakrabarti B, Martin B, Brenner W, Mester J, Clausen M. Adjusted scaling of FDG positron emission tomography images for statistical evaluation in patients with suspected Alzheimer's disease. *J Neuroimaging*. 2005; 15(4):348-55. <http://dx.doi.org/10.1111/j.1552-6569.2005.tb00335.x>. PMID:16254400.
- Byrnes KR, Wilson C, Brabazon F, von Leden R, Jurgens J, Oakes T, Selwyn RG. FDG-PET imaging in mild traumatic brain injury: a critical review. *Front Neuroenergetics*. 2014; 5:13-24. <http://dx.doi.org/10.3389/fnene.2013.00013>. PMID:24409143.
- Carson RE, Channing MA, Blasberg RG, Dunn BB, Cohen RM, Rice KC, Herscovitch P. Comparison of bolus and infusion methods for receptor quantitation: Application to [18F] cyclofoxy and positron emission tomography. *J Cereb Blood Flow Metab*. 1993; 13(1):24-42. <http://dx.doi.org/10.1038/jcbfm.1993.6>. PMID:8380178.
- Casteels C, Martinez E, Bormans G, Camon L, Vera N, Baekelandt V, Planas AM, van Laere K. Type 1 cannabinoid receptor mapping with [18F]MK-9470 PET in the rat brain after quinolinic acid lesion: a comparison to dopamine receptors and glucose metabolism. *Eur J Nucl Med Mol Imaging*. 2010; 37(12):2354-63. <http://dx.doi.org/10.1007/s00259-010-1574-2>. PMID:20680268.
- Casteels C, Vermaelen P, Nuyts J, van der Linden A, Baekelandt V, Mortelmans L, Bormans G, van Laere K. Construction and evaluation of multitracer small-animal PET probabilistic atlases for voxel-based functional mapping of the rat brain. *J Nucl Med*. 2006; 47(11):1858-66. PMID:17079820.
- Catafau AM. Brain SPECT in clinical practice. Part I: perfusion. *J Nucl Med*. 2001; 42(2):259-71. PMID:11216525.
- Chan E, Kovacevic N, Ho SKY, Henkelman RM, Henderson JT. Development of a high resolution three-dimensional surgical atlas of the murine head for strains 129S1/SvImJ and C57Bl/6J using magnetic resonance imaging and micro-computed tomography. *Neuroscience*. 2007; 144(2):604-15. <http://dx.doi.org/10.1016/j.neuroscience.2006.08.080>. PMID:17101233.
- Claeys J, Mertens K, D'Asseler Y, Goethals I. Normoglycemic plasma glucose levels affects F-18 FDG uptake in the brain. *Ann Nucl Med*. 2010; 24(6):501-5. <http://dx.doi.org/10.1007/s12149-010-0359-9>. PMID:20237872.
- Coelho C, Hjernevik T, Courivaud F, Willoch F. Anatomical standardization of small animal brain FDG-PET images using synthetic functional template: experimental comparison with anatomical template. *J Neurosci Methods*. 2011; 199(1):166-72. <http://dx.doi.org/10.1016/j.jneumeth.2011.04.026>. PMID:21550366.
- Convert L, Morin-Brassard G, Cadorette J, Archambault M, Bentourkia M, Lecomte R. A new tool for molecular imaging: the microvolumetric {beta} blood counter. *J Nucl Med*. 2007; 48(7):1197-1206. <http://dx.doi.org/10.2967/jnumed.107.042606>. PMID:17574990.
- Crane PD, Partridge WM, Braun LD, Oldendorf WH. Kinetics of transport and phosphorylation of 2-fluoro-2-deoxy-D-glucose in rat brain. *J Neurochem*. 1983; 40(1):160-7. <http://dx.doi.org/10.1111/j.1471-4159.1983.tb12666.x>. PMID:6848656.
- Crone C. Facilitated transfer of glucose from blood into brain tissue. *J Physiol*. 1965; 181(1):103-13. <http://dx.doi.org/10.1113/jphysiol.1965.sp007748>. PMID:5866278.
- Cui Y, Toyoda H, Sako T, Onoe K, Hayashinaka E, Wada Y, Yokoyama C, Onoe H, Kataoka Y, Watanabe Y. A voxel-based analysis of brain activity in high-order trigeminal pathway in the rat induced by cortical spreading depression. *Neuroimage*. 2015; 108:17-22. <http://dx.doi.org/10.1016/j.neuroimage.2014.12.047>. PMID:25536498.
- Cunnane S, Nugent S, Roy M, Courchesne-Loyer A, Croteau E, Tremblay S, Castellano A, Pifferi F, Bocti C, Paquet N, Begdouri H, Bentourkia M, Turcotte E, Allard M, Barberger-Gateau P, Fulop T, Rapoport SI. Brain fuel metabolism, aging, and Alzheimer's disease. *Nutrition*. 2011; 27(1):3-20. <http://dx.doi.org/10.1016/j.nut.2010.07.021>. PMID:21035308.
- Cunningham VJ, Jones T. Spectral analysis of dynamic PET studies. *J Cereb Blood Flow Metab*. 1993; 13(1):15-23. <http://dx.doi.org/10.1038/jcbfm.1993.5>. PMID:8417003.
- Deleye S, Verhaeghe J, Wyffels L, Dedeurwaerdere S, Stroobants S, Staelens S. Towards a reproducible protocol for repetitive and semi-quantitative rat brain imaging with 18F-FDG: exemplified in a memantine pharmacological challenge. *Neuroimage*. 2014; 96:276-87. <http://dx.doi.org/10.1016/j.neuroimage.2014.04.004>. PMID:24736171.
- Dienel GA. Fueling and imaging brain activation. *ASN Neuro*. 2012; 4(5):267-321. <http://dx.doi.org/10.1042/AN20120021>. PMID:22612861.
- Dukart J, Mueller K, Horstmann A, Vogt B, Frisch S, Barthel H, Becker G, Möller HE, Villringer A, Sabri O, Schroeter ML. Differential effects of global and cerebellar normalization on detection and differentiation of dementia in FDG-PET studies. *Neuroimage*. 2010; 49(2):1490-5. <http://dx.doi.org/10.1016/j.neuroimage.2009.09.017>. PMID:19770055.
- Dukart J, Pernecky R, Förster S, Barthel H, Diehl-Schmid J, Draganski B, Obrig H, Santarnecchi E, Drzezga A, Fellgiebel A, Frackowiak R, Kurz A, Müller S, Sabri O, Schroeter ML,

- Yakushev I. Reference cluster normalization improves detection of frontotemporal lobar degeneration by means of FDG-PET. *PLoS One*. 2013; 8(2):e55415. <http://dx.doi.org/10.1371/journal.pone.0055415>. PMID:23451025.
- Durand E, Besson F. How is the standard uptake value (SUV) linked to the influx constant in Sokoloff's model for 18F-FDG? *Med Nucl (Paris)*. 2015; 39(1):11-7. <http://dx.doi.org/10.1016/j.mednuc.2015.01.002>.
- Fang YH, Muzic R Jr. Spillover and partial-volume correction for image-derived input functions for small-animal 18F-FDG PET studies. *J Nucl Med*. 2008; 49(4):606-14. <http://dx.doi.org/10.2967/jnumed.107.047613>. PMID:18344438.
- Fasihi M, Mikhael W. Overview of current biomedical image segmentation methods. In: International Conference on Computational Science and Computational Intelligence (CSCI); Dec 2016 15-16; Las Vegas. Las Vegas: IEEE; 2016, p. 803-8. doi: <http://dx.doi.org/10.1109/CSCI.2016.0156>.
- Frey EC, Humm J, Ljungberg M. Accuracy and precision of radioactivity quantification in nuclear medicine images. *Semin Nucl Med*. 2012; 42(3):208-18. <http://dx.doi.org/10.1053/j.semnuclmed.2011.11.003>. PMID:22475429.
- Friston K. Statistics I: Experimental design and statistical parametric mapping. In: Toga A, Mazziotta J, editors. *Brain Mapping: The Methods*. 2nd ed. San Diego: Academic Press; 2002. p. 605-10. <http://dx.doi.org/10.1016/B978-012693019-1/50024-1>.
- Friston K. Introduction. In: Friston K, Ashburner J, Kiebel S, Nichols T, Penny W. *Statistical parametric mapping: the analysis of functional brain imaging*. San Diego: Academic Press; 2007. p. 3-9. <http://dx.doi.org/10.1016/B978-012372560-8/50001-2>.
- Friston KJ, Holmes AP, Worsley KJ, Poline J-P, Frith CD, Frackowiak RSJ. Statistical parametric maps in functional imaging: a general linear approach. *Hum Brain Mapp*. 1994; 2(4):189-210. <http://dx.doi.org/10.1002/hbm.460020402>.
- Frumberg DB, Fernando M, Lee D, Biegona A, Schiffer W. Metabolic and behavioral deficits following a routine surgical procedure in rats. *Brain Res*. 2007; 1144:209-18. <http://dx.doi.org/10.1016/j.brainres.2007.01.134>. PMID:17346680.
- Fueger BJ, Czernin J, Hildebrandt I, Tran C, Halpern BS, Stout D, Phelps ME, Weber WA. Impact of animal handling on the results of 18F-FDG PET studies in mice. *J Nucl Med*. 2006; 47(6):999-1006. PMID:16741310.
- Germino M, Gallezot JD, Yan J, Carson RE. Direct reconstruction of parametric images for brain PET with event-by-event motion correction: evaluation in two tracers across count levels. *Phys Med Biol*. 2017; 62(13):5344-64. <http://dx.doi.org/10.1088/1361-6560/aa731f>. PMID:28504644.
- Gispert JD, Pascau J, Reig S, Garcia-Barreno P, Desco M. Mapas de estadísticos paramétricos (SPM) en medicina nuclear. *Rev Esp Med Nucl*. 2003; 22(1):43-53. [http://dx.doi.org/10.1016/S0212-6982\(03\)72141-7](http://dx.doi.org/10.1016/S0212-6982(03)72141-7). PMID:12550034.
- Golla SSV, Adriaanse SM, Yaqub M, Windhorst AD, Lammertsma AA, van Berckel BNM, Boellaard R. Model selection criteria for dynamic brain PET studies. *EJNMMI Phys*. 2017; 4(1):30. <http://dx.doi.org/10.1186/s40658-017-0197-0>. PMID:29209862.
- Green LA, Gambhir SS, Srinivasan A, Banerjee PK, Hoh CK, Cherry SR, Sharfstein S, Barrio JR, Herschman HR, Phelps ME. Noninvasive methods for quantitating blood time-activity curves from mouse PET images obtained with fluorine-18-fluorodeoxyglucose. *J Nucl Med*. 1998; 39(4):729-34. PMID:9544690.
- Gunn RN, Gunn S, Cunningham V. Positron emission tomography compartmental models. *J Cereb Blood Flow Metab*. 2001; 21(6):635-52. <http://dx.doi.org/10.1097/00004647-200106000-00002>. PMID:11488533.
- Gustafson C, Tretiak O, Bertrand L, Nissano J. Design and implementation of software for assembly and browsing of 3D brain atlases. *Comput Methods Programs Biomed*. 2004; 74(1):53-61. [http://dx.doi.org/10.1016/S0169-2607\(03\)00075-0](http://dx.doi.org/10.1016/S0169-2607(03)00075-0). PMID:14992826.
- Hargreaves RJ, Rabiner E. Translational PET imaging research. *Neurobiol Dis*. 2014; 61:32-8. <http://dx.doi.org/10.1016/j.nbd.2013.08.017>. PMID:24055214.
- Huang S, Phelps M. Principles of tracer kinetic modeling in positron emission tomography and autoradiography. In: Mazziotta J, Phelps M, Schelbert H editors. *Positron Emission Tomography and Autoradiography*. Philadelphia: Raven Press; 1985. p. 287-346.
- Huang S-C, Wong K-P. Dynamic PET imaging. In: M Dahlbom, editor. *Physics of PET and SPECT imaging: Imaging in medical diagnosis and therapy*. Boca Raton: CRC Press, Taylor & Francis Group; 2017. p. 321-36. <http://dx.doi.org/10.1201/9781315374383-16>.
- Huang SC. Anatomy of SUV: Standardized Uptake Value. *Nucl Med Biol*. 2000; 27(7):643-6. [http://dx.doi.org/10.1016/S0969-8051\(00\)00155-4](http://dx.doi.org/10.1016/S0969-8051(00)00155-4). PMID:11091106.
- Ido T, Wan CN, Casella V, Fowler J, Wolf A, Reivich M, Kuhl DE. Labeled 2-deoxy-D-glucose analogs. 18F-labeled 2-deoxy-2-fluoro-D-glucose, 2-deoxy-2-fluoro-D-mannose and 14C-2-deoxy-2-fluoro-D-glucose. *J Labelled Comp Radiopharm*. 1978; 14(2):175-83. <http://dx.doi.org/10.1002/jlcr.2580140204>.
- Ingvar D. Mental-illness and regional brain metabolism. *Trends Neurosci*. 1982; 5:199-203. [http://dx.doi.org/10.1016/0166-2236\(82\)90114-X](http://dx.doi.org/10.1016/0166-2236(82)90114-X).
- Ishizu K, Nishizawa S, Yonekura Y, Sadato N, Magata Y, Tamaki N, Tsuchida T, Okazawa H, Miyatake S, Ishikawa M, et al. Effects of hyperglycemia on FDG uptake in human brain and glioma. *J Nucl Med*. 1994; 35(7):1104-9. PMID:8014665.
- Jadvar H, Parker J. PET radiotracers. In: Jadvar H, Parker J editors. *Clinical PET and PET/CT*. London: Springer; 2005. p. 45-67.
- Jagoda EM, Vaquero J, Seidel J, Green M, Eckelman W. Experiment assessment of mass effects in the rat: implications for small animal PET imaging. *Nucl Med Biol*. 2004; 31(6):771-9. <http://dx.doi.org/10.1016/j.nucmedbio.2004.04.003>. PMID:15246368.
- Jensen TL, Kiersgaard MK, Sorensen DB, Mikkelsen LF. Fasting of mice: a review. *Lab Anim*. 2013; 47(4):225-40. <http://dx.doi.org/10.1177/0023677213501659>. PMID:24025567.
- Karsch K, He Q, Duan Y. A fast, semiautomatic brain structure segmentation algorithm for magnetic resonance imaging.

- In: IEEE International Conference on Bioinformatics and Biomedicine; 2009 Nov 1-4; Washington, DC. Washington: IEEE Computer Society; 2009. p. 297-302. DOI: 10.1109/BIBM.2009.40.
- Kawasaki K, Ishii K, Saito Y, Oda K, Kimura Y, Ishiwata K. Influence of mild hyperglycemia on cerebral FDG distribution patterns calculated by statistical parametric mapping. *Ann Nucl Med*. 2008; 22(3):191-200. <http://dx.doi.org/10.1007/s12149-007-0099-7>. PMID:18498034.
- Keramida G, Anagnostopoulos C, Peters M. The extent to which standardized uptake values reflect FDG phosphorylation in the liver and spleen as functions of time after injection of 18F-fluorodeoxyglucose. *EJNMMI Res*. 2017; 7(1):13. <http://dx.doi.org/10.1186/s13550-017-0254-7>. PMID:28176243.
- Kim J, Herrero P, Sharp T, Laforest R, Rowland DJ, Tai Y-C, Lewis JS, Welch MJ. Minimally invasive method of determining blood input function from PET images in rodents. *J Nucl Med*. 2006; 47(2):330-6. PMID:16455640.
- Knol RJ, de Bruin K, de Jong J, van Eck-Smit B, Booij J. *In vitro* and *ex vivo* storage phosphor imaging of short-living radioisotopes. *J Neurosci Methods*. 2008; 168(2):341-57. <http://dx.doi.org/10.1016/j.jneumeth.2007.10.028>. PMID:18164072.
- Köroğlu R, Köksal İ, Şimşek FS, Gezer F, Kekilli E, Ünal B. Considering the relationship between quantitative parameters and prognostic factors in breast cancer: can mean standardized uptake value be an alternative to maximum standardized uptake value? *World J Nucl Med*. 2017; 16(4):275-80. <http://dx.doi.org/10.4103/1450-1147.215485>. PMID:29033675.
- Kotasidis F, Tsoumpas C, Rahmim A. Advanced kinetic modeling strategies: towards adoption in clinical PET imaging. *Clin Transl Imaging*. 2014; 2(3):219-37. <http://dx.doi.org/10.1007/s40336-014-0069-8>.
- Krak NC, Boellaard R, Hoekstra O, Twisk J, Hoekstra C, Lammertsma A. Effects of ROI definition and reconstruction method on quantitative outcome and applicability in a response monitoring trial. *Eur J Nucl Med Mol Imaging*. 2005; 32(3):294-301. <http://dx.doi.org/10.1007/s00259-004-1566-1>. PMID:15791438.
- Krohn KA, Muzi MSA, Spence AM. What is in a number? The FDG lumped constant in the rat brain. *J Nucl Med*. 2007; 48(1):5-7. PMID:17204692.
- Kung M-P, Kung H. Mass effect of injection dose in small rodent imaging by SPECT and PET. *Nucl Med Biol*. 2005; 32(7):673-8. <http://dx.doi.org/10.1016/j.nucmedbio.2005.04.002>. PMID:16243641.
- Kyme AZ, Zhou VW, Meikle SR, Baldock C, Fulton RR. Optimized motion tracking for positron emission tomography studies of brain function in awake rats. *PLoS One*. 2011; 6(7):e21727. <http://dx.doi.org/10.1371/journal.pone.0021727>. PMID:21747951.
- Lein ES, Hawrylycz MJ, Ao N, Ayres M, Bensinger A, Bernard A, Boe AF, Boguski MS, Brockway KS, Byrnes EJ, Chen L, Chen L, Chen T-M, Chi Chin M, Chong J, Crook BE, Czaplinska A, Dang CN, Datta S, Dee NR, Desaki AL, Desta T, Diep E, Dolbeare TA, Donelan MJ, Dong H-W, Dougherty JG, Duncan BJ, Ebbert AJ, Eichele G, Estlin LK, Faber C, Facer BA, Fields R, Fischer SR, Fliss TP, Frensley C, Gates SN, Glattfelder KJ, Halverson KR, Hart MR, Hohmann JG, Howell MP, Jeung DP, Johnson RA, Karr PT, Kawal R, Kidney JM, Knapik RH, Kuan CL, Lake JH, Laramee AR, Larsen KD, Lau C, Lemon TA, Liang AJ, Liu Y, Luong LT, Michaels J, Morgan JJ, Morgan RJ, Mortrud MT, Mosqueda NF, Ng LL, Ng R, Orta GJ, Overly CC, Pak TH, Parry SE, Pathak SD, Pearson OC, Puchalski RB, Riley ZL, Rockett HR, Rowland SA, Royall JJ, Ruiz MJ, Sarno NR, Schaffnit K, Shapovalova NV, Sivisay T, Slaughterbeck CR, Smith SC, Smith KA, Smith BI, Sotd AJ, Stewart NN, Stumpf K-R, Sunkin SM, Sutram M, Tam A, Teemer CD, Thaller C, Thompson CL, Varnam LR, Visel A, Whitlock RM, Wohnoutka PE, Wolkey CK, Wong VY, Wood M, Yaylaoglu MB, Young RC, Youngstrom BL, Feng Yuan X, Zhang B, Zwingman TA, Jones AR. Genome-wide atlas of gene expression in the adult mouse brain. *Nature*. 2007; 445(7124):168-76. <http://dx.doi.org/10.1038/nature05453>. PMID:17151600.
- Leybaert L, De Bock M, van Moorchem M, Decroock E, de Vuyst E. Neurobarrier coupling in the brain: adjusting glucose entry with demand. *J Neurosci Res*. 2007; 85(15):3213-20. <http://dx.doi.org/10.1002/jnr.21189>. PMID:17265466.
- Litaudon P, Bouillot C, Zimmer L, Costes N, Ravel N. Activity in the rat olfactory cortex is correlated with behavioral response to odor: a microPET study. *Brain Struct Funct*. 2017; 222(1):577-86. <http://dx.doi.org/10.1007/s00429-016-1235-8>. PMID:27194619.
- MacKenzie-Graham A, Lee EF, Dinov ID, Bota M, Shattuck DW, Ruffins S, Yuan H, Konstantinidis F, Pitiot A, Ding Y, Hu G, Jacobs RE, Toga AW. A multimodal, multidimensional atlas of the C57BL/6J mouse brain. *J Anat*. 2004; 204(2):93-102. <http://dx.doi.org/10.1111/j.1469-7580.2004.00264.x>. PMID:15032916.
- Matsumura A, Mizokawa S, Tanaka M, Wada Y, Nozaki S, Nakamura F, Shiomi S, Ochi H, Watanabe Y. Assessment of microPET performance in analyzing the rat brain under different types of anesthesia: comparison between quantitative data obtained with microPET and *ex vivo* autoradiography. *Neuroimage*. 2003; 20(4):2040-50. <http://dx.doi.org/10.1016/j.neuroimage.2003.08.020>. PMID:14683708.
- McLaughlin KJ, Gomez JL, Baran SE, Conrad CD. The effects of chronic stress on hippocampal morphology and function: an evaluation of chronic restraint paradigms. *Brain Res*. 2007; 1161(1):56-64. <http://dx.doi.org/10.1016/j.brainres.2007.05.042>. PMID:17603026.
- Meyer M, Le-Bras L, Fernandez P, Zanotti-Fregonara P. Standardized input function for 18F-FDG PET studies in mice: a cautionary study. *PLoS One*. 2017; 12(1):e0168667. <http://dx.doi.org/10.1371/journal.pone.0168667>. PMID:28125579.
- Meyer PT, Circiumaru V, Cardi CA, Thomas DH, Bal H, Acton PD. Simplified quantification of small animal [18F]FDG PET studies using a standard arterial input function. *Eur J Nucl Med Mol Imaging*. 2006; 33(8):948-54. <http://dx.doi.org/10.1007/s00259-006-0121-7>. PMID:16699768.
- Mizuma H, Shukuri M, Hayashi T, Watanabe Y, Onoe H. Establishment of *in vivo* brain imaging method in conscious mice. *J Nucl Med*. 2010; 51(7):1068-75. <http://dx.doi.org/10.2967/jnumed.110.075184>. PMID:20554730.

- Moore AH, Osteen C, Chatziioannou A, Hovda D, Cherry S. Quantitative assessment of longitudinal metabolic changes *in vivo* after traumatic brain injury in the adult rat using FDG-microPET. *J Cereb Blood Flow Metab.* 2000; 20(10):1492-501. <http://dx.doi.org/10.1097/00004647-200010000-00011>. PMID:11043912.
- Munk OL, Keiding S, Bass L. A method to estimate dispersion in sampling catheters and to calculate dispersion-free blood time-activity curves. *Med Phys.* 2008; 35(8):3471-81. <http://dx.doi.org/10.1118/1.2948391>. PMID:18777907.
- Nehlig A. Cerebral energy metabolism, glucose transport and blood flow: changes with maturation and adaptation to hypoglycaemia. *Diabetes Metab.* 1997; 23(1):18-29. PMID:9059763.
- Nie B, Chen K, Zhao S, Liu J, Gu X, Yao Q, Hui J, Zhang Z, Teng G, Zhao C, Shan B. A rat brain MRI template with digital stereotaxic atlas of fine anatomical delineations in paxinos space and its automated application in voxel-wise analysis. *Hum Brain Mapp.* 2013; 34(6):1306-18. <http://dx.doi.org/10.1002/hbm.21511>. PMID:22287270.
- Nie B, Liu H, Chen K, Jiang X, Shan B. A statistical parametric mapping toolbox used for voxel-wise analysis of FDG-PET images of rat brain. *PLoS One.* 2014; 9(9):e108295. <http://dx.doi.org/10.1371/journal.pone.0108295>. PMID:25259529.
- Orzi F, Lucignani G, Dow-Edwards D, Namba H, Nehlig A, Patlak CS, Pettigrew K, Schuier F, Sokoloff L. Local cerebral glucose utilization in controlled graded levels of hyperglycemia in the conscious rat. *J Cereb Blood Flow Metab.* 1988; 8(3):346-56. <http://dx.doi.org/10.1038/jcbfm.1988.70>. PMID:3366796.
- Paquet N, Albert A, Foidart J, Hustinx R. Within-patient variability of ¹⁸F-FDG: standardized uptake values in normal tissues. *J Nucl Med.* 2004; 45(5):784-8. PMID:15136627.
- Park TY, Nishida KS, Wilson CM, Jaiswal S, Scott J, Hoy AR, Selwyn RG, Dardzinski BJ, Choi KH. Effects of isoflurane anesthesia and intravenous morphine self-administration on regional glucose metabolism ([¹⁸F]FDG-PET) of male Sprague-Dawley rats. *Eur J Neurosci.* 2017; 45(7):922-31. <http://dx.doi.org/10.1111/ejn.13542>. PMID:28196306.
- Patlak CS, Blasberg R, Fenstermacher J. Graphical evaluation of blood-to-brain transfer constants from multiple-time uptake data. *J Cereb Blood Flow Metab.* 1983; 3(1):1-7. <http://dx.doi.org/10.1038/jcbfm.1983.1>. PMID:6822610.
- Patlak CS, Blasberg R. Graphical evaluation of blood-to-brain transfer constants from multiple-time uptake data. Generalizations. *J Cereb Blood Flow Metab.* 1985; 5(4):584-90. <http://dx.doi.org/10.1038/jcbfm.1985.87>. PMID:4055928.
- Paxinos G, Watson C. *The rat brain in stereotaxic coordinates: compact.* 7th ed. San Diego: Elsevier Academic Press; 2017.
- Phelps ME, Huang SC, Hoffman EJ, Selin C, Sokoloff L, Kuhl DE. Tomographic measurement of local cerebral glucose metabolic rate in man with (¹⁸F) fluorodeoxyglucose: Validation of method. *Ann Neurol.* 1979; 6(5):371-88. <http://dx.doi.org/10.1002/ana.410060502>. PMID:117743.
- Poussier S, Maskali F, Vexiau G, Verger A, Boutley H, Karcher G, Raffo E, Marie PY. Quantitative SPM analysis involving an adaptive template may be applied to [¹⁸F]FDG PET images of the rat brain. *Mol Imaging Biol.* 2017; 19(5):731-5. <http://dx.doi.org/10.1007/s11307-016-1043-9>. PMID:28108871.
- Reimold M, Slifstein M, Heinz A, Mueller-Schauenburg W, Bares R. Effect of spatial smoothing on t-maps: arguments for going back from t-maps to masked contrast images. *J Cereb Blood Flow Metab.* 2006; 26(6):751-9. <http://dx.doi.org/10.1038/sj.jcbfm.9600231>. PMID:16208316.
- Roy CS, Sherrington C. On the Regulation of the blood-supply of the brain. *J Physiol.* 1890; 11(1-2):85-158, 17. <http://dx.doi.org/10.1113/jphysiol.1890.sp000321>. PMID:16991945.
- Sapienza M, Buchpiguel CA. Bases da tomografia por emissão de pósitrons (PET). In Hironaka F, Sapienza M, Ono C, Lima M, Buchpiguel C, editors. *Medicina nuclear: princípios e aplicações.* 2nd ed. Rio de Janeiro: Atheneu; 2017. p. 372-7.
- Schiffer WK, Mirrione M, Dewey S. Optimizing experimental protocols for quantitative behavioral imaging with ¹⁸F-FDG in rodents. *J Nucl Med.* 2007; 48(2):277-87. PMID:17268026.
- Schmidt KC, Smith C. Resolution, sensitivity and precision with autoradiography and small animal positron emission tomography: implications for functional brain imaging in animal research. *Nucl Med Biol.* 2005; 32(7):719-25. <http://dx.doi.org/10.1016/j.nucmedbio.2005.04.020>. PMID:16243647.
- Schuier F, Orzi F, Suda S, Lucignani G, Kennedy C, Sokoloff L. Influence of plasma glucose concentration on lumped constant of the deoxyglucose method: effects of hyperglycemia in the rat. *J Cereb Blood Flow Metab.* 1990; 10(6):765-73. <http://dx.doi.org/10.1038/jcbfm.1990.134>. PMID:2211874.
- Schulz D, Southekal S, Junnarkar SS, Pratte JF, Purschke ML, Stoll SP, Ravindranath B, Maramraju SH, Krishnamoorthy S, Henn FA, O'Connor P, Woody CL, Schlyer DJ, Vaska P. Simultaneous assessment of rodent behavior and neurochemistry using a miniature positron emission tomograph. *Nat Methods.* 2011; 8(4):347-52. <http://dx.doi.org/10.1038/nmeth.1582>. PMID:21399637.
- Schwarz AJ, Danckaert A, Reese T, Gozzi A, Paxinos G, Watson C, Merlo-Pich EV, Bifone A. A stereotaxic MRI template set for rat brain with tissue class distribution maps and co-registered anatomical atlas: application to pharmacological MRI. *Neuroimage.* 2006; 32(2):538-50. <http://dx.doi.org/10.1016/j.neuroimage.2006.04.214>. PMID:16784876.
- Schweinhart P, Fransson P, Olson L, Spenger C, Andersson J. A template for spatial normalisation of MR images of the rat brain. *J Neurosci Methods.* 2003; 129(2):105-13. [http://dx.doi.org/10.1016/S0165-0270\(03\)00192-4](http://dx.doi.org/10.1016/S0165-0270(03)00192-4). PMID:14511814.
- Senda M, Nishizawa S, Yonekura Y, Mukai T, Saji H, Konishi J, Torizuka K. Measurement of arterial time-activity curve by monitoring continuously drawn arterial blood with an external detector: errors and corrections. *Ann Nucl Med.* 1988; 2(1):7-12. <http://dx.doi.org/10.1007/BF03164580>. PMID:3275106.
- Sijbesma JW, Zhou X, Vázquez García D, Houwertjes MC, Doorduyn J, Kwizera C, Maas B, Meerlo P, Dierckx RA, Slart RH, Elsinga PH, van Waarde A. Novel approach to repeated arterial blood sampling in small animal PET: application in a test-retest study with the adenosine A1 receptor ligand [¹¹C]MPDX. *Mol Imaging Biol.* 2016; 18(5):715-23. <http://dx.doi.org/10.1007/s11307-016-0954-9>. PMID:27091332.

- Silva-Rodríguez J, Aguiar P, Domínguez-Prado I, Fierro P, Ruibal Á. Simulated FDG-PET studies for the assessment of SUV quantification methods. *Rev Esp Med Nucl Imagen Mol.* 2015; 34(1):13-8. <http://dx.doi.org/10.1016/j.remnm.2014.07.006>. PMID:25107595.
- Silverman DH. Brain 18F-FDG PET in the diagnosis of neurodegenerative dementias: comparison with perfusion SPECT and with clinical evaluations lacking nuclear imaging. *J Nucl Med.* 2004; 45(4):594-607. PMID:15073255.
- Sokoloff L, Reivich M, Kennedy C, Rosiers MHD, Patlak CS, Pettigrew KD, Sakurada O, Shinohara M. The [14C] deoxyglucose method for the measurement of local cerebral glucose utilization: theory, procedure, and normal values in the conscious and anesthetized albino rat. *J Neurochem.* 1977; 28(5):897-16. <http://dx.doi.org/10.1111/j.1471-4159.1977.tb10649.x>. PMID:864466.
- Sokoloff L. Localization of functional activity in the central nervous system by measurement of glucose utilization with radioactive deoxyglucose. *J Cereb Blood Flow Metab.* 1981b; 1(1):7-36. <http://dx.doi.org/10.1038/jcbfm.1981.4>. PMID:7035471.
- Sokoloff L. The deoxyglucose method: theory and practice. *Eur Neurol.* 1981a; 20(3):137-45. <http://dx.doi.org/10.1159/000115222>. PMID:7262108.
- Solon EG. Autoradiography techniques and quantification of drug distribution. *Cell Tissue Res.* 2015; 360(1):87-107. <http://dx.doi.org/10.1007/s00441-014-2093-4>. PMID:25604842.
- Sossi V, Ruth T. MicroPET imaging: *in vivo* biochemistry in small animals. *J Neural Transm.* 2005; 112(3):319-30. <http://dx.doi.org/10.1007/s00702-004-0272-2>. PMID:15723157.
- Spangler-Bickell MG, de Laat B, Fulton R, Bormans G, Nuyts J. The effect of isoflurane on 18F-FDG uptake in the rat brain: a fully conscious dynamic PET study using motion compensation. *EJNMMI Res.* 2016; 6(1):86. <http://dx.doi.org/10.1186/s13550-016-0242-3>. PMID:27888500.
- Spence A, Muzi M, Graham M, O'Sullivan F, Krohn K, Link J, Lewellen TK, Lewellen B, Freeman SD, Berger MS, Ojemann GA. Glucose metabolism in human malignant gliomas measured quantitatively with PET, 1-[C-11]glucose and FDG: analysis of the FDG lumped constant. *J Nucl Med.* 1998; 39(3):440-8. PMID:9529289.
- Stout D, Pastuskovas C. *In vitro* methods for *in vivo* quantitation of PET and SPECT imaging probes: autoradiography and gamma counting. In: Kiessling F, Pichler BJ, editors. *Small animal imaging: basics and practical guide*. 2nd ed. Heidelberg: Springer; 2011. p. 511-25. http://dx.doi.org/10.1007/978-3-642-12945-2_24.
- Strauss LG, Pan L, Cheng C, Haberkorn U, Dimitrakopoulou-Strauss A. Shortened acquisition protocols for the quantitative assessment of the 2-tissue-compartment model using dynamic PET/CT 18F-FDG studies. *J Nucl Med.* 2011; 52(3):379-85. <http://dx.doi.org/10.2967/jnumed.110.079798>. PMID:21321263.
- Suda S, Shinohara M, Miyaoka M, Lucignani G, Kennedy C, Sokoloff L. The lumped constant of the deoxyglucose method in hypoglycemia: effects of moderate hypoglycemia on local cerebral glucose utilization in the rat. *J Cereb Blood Flow Metab.* 1990; 10(4):499-509. <http://dx.doi.org/10.1038/jcbfm.1990.92>. PMID:2347881.
- Sugawara Y, Zasadny K, Grossman H, Francis I, Clarke M, Wahl R. Germ cell tumor: differentiation of viable tumor, mature teratoma, and necrotic tissue with FDG PET and kinetic modeling. *Radiology.* 1999; 211(1):249-56. <http://dx.doi.org/10.1148/radiology.211.1.r99ap16249>. PMID:10189480.
- Sung KK, Jang DP, Lee S, Kim M, Lee SY, Kim YB, Park CW, Cho ZH. Neural responses in rat brain during acute immobilization stress: a [18F]FDG micro PET imaging study. *Neuroimage.* 2009; 44(3):1074-80. PMID:18952183. doi: 10.1016/j.neuroimage.2008.09.032.
- Swanson LW. *Brain maps: structure of the rat brain*. San Diego: Elsevier Academic Press; 2004.
- Takikawa S, Dhawan V, Spetsieris P, Robeson W, Chaly T, Dahl R, Margoulef D, Eidelberg D. Noninvasive quantitative fluorodeoxyglucose PET studies with an estimated input function derived from a population-based arterial blood curve. *Radiology.* 1993; 188(1):131-6. <http://dx.doi.org/10.1148/radiology.188.1.8511286>. PMID:8511286.
- This JA. Clarification of a fractional uptake concept. *J Nucl Med.* 1995; 36(4):711-2. PMID:7699475.
- Toyama H, Ichise M, Liow JS, Vines D, Seneca N, Modell K, Seidel J, Green MV, Innis RB. Evaluation of anesthesia effects on [18F]FDG uptake in mouse brain and heart using small animal PET. *Nucl Med Biol.* 2004; 31(2):251-6. [http://dx.doi.org/10.1016/S0969-8051\(03\)00124-0](http://dx.doi.org/10.1016/S0969-8051(03)00124-0). PMID:15013491.
- Tsukada H. Animal PET research with non-human primates for drug development in pre-clinical stage - The Hamamatsu experience. In: Elsinga PH, Waarde A van, Paans AMJ, Dierckx RAJO, editors. *Trends on the role of PET in drug development*. Singapore: World Scientific; 2012. p. 241-60. http://dx.doi.org/10.1142/9789814317740_0010.
- Tylski P, Stute S, Grotus N, Doyeux K, Hapdey S, Gardin I, Vanderlinden B, Buvat I. Comparative assessment of methods for estimating tumor volume and standardized uptake value in (18)F-FDG PET. *J Nucl Med.* 2010; 51(2):268-76. <http://dx.doi.org/10.2967/jnumed.109.066241>. PMID:20080896.
- Vállez García D, Casteels C, Schwarz A, Dierckx R, Koole M, Doorduyn J. A standardized method for the construction of tracer specific PET and SPECT rat brain templates: validation and implementation of a toolbox. *PLoS One.* 2015; 10(3):e0122363. <http://dx.doi.org/10.1371/journal.pone.0122363>. PMID:25823005.
- van den Hoff J. Kinetic modeling. In: Kiessling F, Pichler BJ, editors. *Small animal imaging: basics and practical guide*. 2nd ed. Heidelberg: Springer; 2011. p. 559-80. http://dx.doi.org/10.1007/978-3-642-12945-2_27.
- Vanhove C, Bankstahl J, Krämer S, Visser E, Belcari N, Vandenberghe S. Accurate molecular imaging of small animals taking into account animal models, handling, anaesthesia, quality control and imaging system performance. *EJNMMI Phys.* 2015; 2(1):31. <http://dx.doi.org/10.1186/s40658-015-0135-y>. PMID:26560138.
- Vaska P, Woody CL, Schlyer DJ, Shokouhi S, Stoll SP, Pratte JF et al. RatCAP: miniaturized head-mounted PET for conscious rodent brain imaging. *IEEE Trans Nucl Sci.* 2004; 51(5 II):2718-22. doi:10.1109/NSSMIC.2003.1352223.
- Veronese M, Rizzo G, Bertoldo A, Turkheimer FE. Spectral analysis of dynamic PET studies: a review of 20 years of method

- developments and applications. *Comput Math Methods Med.* 2016; 2016:1-15. <http://dx.doi.org/10.1155/2016/7187541>. PMID:28050197.
- Viglianti BL, Wong K, Wimer S, Parameswaran A, Nan B, Ky C, Townsend DM, Rubello D, Frey KA, Gross MD. Effect of hyperglycemia on brain and liver 18F-FDG standardized uptake value (FDG SUV) measured by quantitative positron emission tomography (PET) imaging. *Biomed Pharmacother.* 2017; 88:1038-45. <http://dx.doi.org/10.1016/j.biopha.2017.01.166>. PMID:28192877.
- Wang G, Qi J. Direct estimation of kinetic parametric images for dynamic PET. *Theranostics.* 2013; 3(10):802-15. <http://dx.doi.org/10.7150/thno.5130>. PMID:24396500.
- Weber B, Burger C, Biro P, Buck A. A femoral arteriovenous shunt facilitates arterial whole blood sampling in animals. *Eur J Nucl Med Mol Imaging.* 2002; 29(3):319-23. <http://dx.doi.org/10.1007/s00259-001-0712-2>. PMID:12002705.
- Weber WA, Ziegler S, Thodtmann R, Hanauske AR, Schwaiger M. Reproducibility of metabolic measurements in malignant tumors using FDG PET. *J Nucl Med.* 1999; 40(11):1771-7. PMID:10565769.
- Weisenberger AG, Gleason SS, Goddard J, Kross B, Majewski S, Meikle SR. A restraint-free small animal SPECT imaging system with motion tracking. *IEEE Trans Nucl Sci.* 2005; 52(31):638-44. doi:10.1109/TNS.2005.851399.
- Welch A, Mingarelli M, Riedel G, Platt B. Mapping changes in mouse brain metabolism with PET/CT. *J Nucl Med.* 2013; 54(11):1946-53. <http://dx.doi.org/10.2967/jnumed.113.121509>. PMID:24009277.
- White DRR, Houston A, Sampson W, Wilkins G. Intra-and interoperator variations in region-of-interest drawing and their effect on the measurement of glomerular filtration rates. *Clin Nucl Med.* 1999; 24(3):177-81. <http://dx.doi.org/10.1097/00003072-199903000-00008>. PMID:10069728.
- Yakushev I, Hammers A, Fellgiebel A, Schmidtman I, Scheurich A, Buchholz H-G, Peters J, Bartenstein P, Lieb K, Schreckenberger M. SPM-based count normalization provides excellent discrimination of mild Alzheimer's disease and amnesic mild cognitive impairment from healthy aging. *Neuroimage.* 2009; 44(1):43-50. <http://dx.doi.org/10.1016/j.neuroimage.2008.07.015>. PMID:18691659.
- Zanotti-Fregonara P, Chen K, Liow JS, Fujita M, Innis RB. Image derived input function for brain PET studies: many challenges and few opportunities. *J Cereb Blood Flow Metab.* 2011; 31(10):1986-98. <http://dx.doi.org/10.1038/jcbfm.2011.107>. PMID:21811289.
- Zanotti-Fregonara P, Fadaili IM, Maroy R, Comtat C, Souloumiac A, Jan S, Ribeiro MJ, Gaura V, Bar-Hen A, Trébossen R. Comparison of eight methods for the estimation of the image-derived input function in dynamic [(18)F]-FDG PET human brain studies. *J Cereb Blood Flow Metab.* 2009; 29(11):1825-35. <http://dx.doi.org/10.1038/jcbfm.2009.93>. PMID:19584890.
- Zanotti-Fregonara P, Hirvonen J, Lyoo CH, Zoghbi SS, Rallis-Frutos D, Huestis MA, Morse C, Pike VW, Innis RB. Population-based input function modeling for [18F]FMPEP-d2, an inverse agonist radioligand for cannabinoid CB1 receptors: validation in clinical studies. *PLoS One.* 2013; 8(4):e60231. <http://dx.doi.org/10.1371/journal.pone.0060231>. PMID:23577094.
- Zanotti-Fregonara P, Liow JS, Comtat C, Zoghbi SS, Zhang Y, Pike VW, Fujita M, Innis RB. Image-derived input function in PET brain studies: blood-based methods are resistant to motion artifacts. *Nucl Med Commun.* 2012; 33(9):982-9. <http://dx.doi.org/10.1097/MNM.0b013e328356185c>. PMID:22760300.